



Stability of zirconium silicate films on Si under vacuum and O₂ annealing

J. Morais, E. B. O. da Rosa, L. Miotti, R. P. Pezzi, I. J. R. Baumvol, A. L. P. Rotondaro, M. J. Bevan, and L. Colombo

Citation: [Applied Physics Letters](#) **78**, 2446 (2001); doi: 10.1063/1.1367288

View online: <http://dx.doi.org/10.1063/1.1367288>

View Table of Contents: <http://scitation.aip.org/content/aip/journal/apl/78/17?ver=pdfcov>

Published by the [AIP Publishing](#)

Articles you may be interested in

[Thermal decomposition behavior of the HfO₂ / SiO₂ / Si system](#)

J. Appl. Phys. **94**, 928 (2003); 10.1063/1.1578525

[Effect of N₂ annealing on AlZrO oxide](#)

J. Vac. Sci. Technol. A **21**, 1482 (2003); 10.1116/1.1586276

[Thermally induced Zr incorporation into Si from zirconium silicate thin films](#)

Appl. Phys. Lett. **79**, 2958 (2001); 10.1063/1.1415418

[Composition, atomic transport, and chemical stability of ZrAl_xO_y ultrathin films deposited on Si\(001\)](#)

Appl. Phys. Lett. **79**, 1998 (2001); 10.1063/1.1405808

[Structure and stability of ultrathin zirconium oxide layers on Si\(001\)](#)

Appl. Phys. Lett. **76**, 436 (2000); 10.1063/1.125779

The image shows the cover of an Applied Physics Reviews journal issue. It features a blue and orange color scheme with a molecular structure background. The text 'NEW Special Topic Sections' is prominently displayed in white. Below it, 'NOW ONLINE' is written in orange, followed by the title 'Lithium Niobate Properties and Applications: Reviews of Emerging Trends' in white. The AIP Applied Physics Reviews logo is in the bottom right corner.

NEW Special Topic Sections

NOW ONLINE
Lithium Niobate Properties and Applications:
Reviews of Emerging Trends

AIP Applied Physics
Reviews

Stability of zirconium silicate films on Si under vacuum and O₂ annealing

J. Morais,^{a)} E. B. O. da Rosa, L. Miotti, R. P. Pezzi, and I. J. R. Baumvol
Instituto de Física, Universidade Federal do Rio Grande do Sul, Av. Bento Gonçalves, 9500-Porto Alegre, 91509-900 Brazil

A. L. P. Rotondaro, M. J. Bevan, and L. Colombo
Silicon Technology Development, Texas Instruments Incorporated, Dallas, Texas 75241

(Received 11 December 2000; accepted for publication 21 February 2001)

The effect of postdeposition annealing in vacuum and in dry O₂ on the atomic transport and chemical stability of chemical vapor deposited ZrSi_xO_y films on Si is investigated. Rutherford backscattering spectrometry, narrow nuclear resonance profiling, and low energy ion scattering spectroscopy were used to obtain depth distributions of Si, O, and Zr in the films. The chemical environment of these elements in near-surface and near-interface regions was identified by angle-resolved x-ray photoelectron spectroscopy. It is shown that although the interface region is rather stable, the surface region presents an accumulation of Si after thermal annealing. © 2001 American Institute of Physics. [DOI: 10.1063/1.1367288]

There is an impetus to replace SiO₂ as the gate dielectric in complementary metal oxide semiconductor (CMOS) transistors, since the exponential increase in tunnel current with decreasing film thickness sets a fundamental limit on the scaling of gate oxides.^{1,2} The trend in reducing lateral dimensions of devices brings as a consequence a reduction of the capacitance of the involved MOS structures, thus calling for a higher dielectric constant and/or thinner films to compensate. Therefore, to keep device areas small and prevent leakage current while maintaining the same gate capacitance, a thicker film made with a material of higher dielectric constant (high-*K*) is required. Further mandatory requirements are: a sharp interface with Si substrate which would favor a low density of interface states; and physico-chemical stability at both the gate electrode/high-*K* dielectric and the high-*K* dielectric/Si-substrate interfaces in further processing steps. Previous investigations³⁻⁸ indicated that a postdeposition annealing at moderate temperatures of thin films of different proposed dielectrics on Si may reduce the leakage current and the density of interface states down to acceptable levels of less than 10⁻¹¹/cm²eV. This was achieved in many cases without a significant lowering of the dielectric constant due to formation of intermediate SiO₂ layers.

Recent publications^{4,5,7} showed that Zr silicates (ZrSi_xO_y), which are stable in direct contact with Si,⁹ are good candidates for alternative, high-*K* dielectrics.

We report on atomic transport and chemical stability of ZrSi_xO_y films submitted to post-deposition thermal anneals in a vacuum and in dry O₂. Zr silicate films, ~9 nm thick, were deposited by low pressure chemical vapor deposition at 650 °C. The postdeposition anneals were performed *ex situ* at 600 °C for 30 min, either in high vacuum ($P = 10^{-5}$ Pa) or in 7×10^3 Pa of dry O₂ 98.5% enriched in the ¹⁸O isotope (¹⁸O₂). Annealing in isotopically enriched O allows distinguishing O eventually incorporated from that previously existing in the silicate films.

Zr profiles and areal densities were determined by Rutherford backscattering spectrometry (RBS) of 700 keV He⁺ ions, detected at a scattering angle of 165° and tilting the sample by 70°. The depth resolution for Zr profiling obtained with this geometry is ~2 nm. RBS geometry and spectra for as-deposited and annealed samples are shown in Fig. 1(a), indicating a uniform and stable (after thermal annealing) distribution of Zr within the silicate film and sharp interfaces with the Si substrate. Areal densities of ¹⁶O, ¹⁸O,

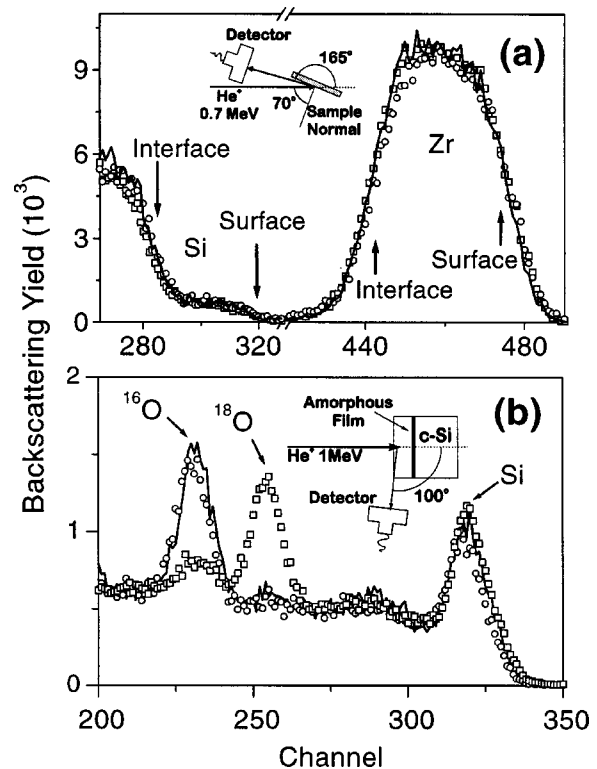


FIG. 1. (a) Zr and Si signals in RBS spectra of 700 keV incident He⁺ ions; (b) channelled-RBS and grazing angle detection spectra of 1 MeV incident He⁺ ions. The geometries are shown in the insets. Solid lines represent the as-deposited sample, empty circles and squares represent the vacuum- and ¹⁸O₂-annealed samples, respectively.

^{a)}Electronic mail: jonder@if.ufrgs.br

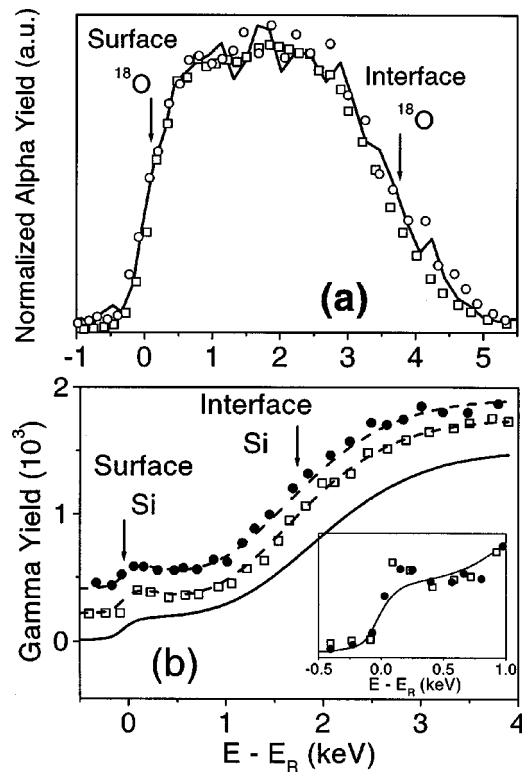


FIG. 2. (a) Normalized excitation curves of the nuclear reaction $^{18}\text{O}(p,\alpha)^{15}\text{N}$ around the resonance at 151 keV. The normalization consisted in dividing the excitation curve for the $^{18}\text{O}_2$ -annealed sample by 380. (b) Excitation curves of the nuclear reaction $^{29}\text{Si}(p,\gamma)^{30}\text{P}$ around the resonance at 414 keV. The inset shows the region of the excitation curves corresponding to the surface. Symbols are the same as in Fig. 1.

and Si were determined by RBS in a channeling geometry:¹⁰ 1 MeV He^+ ions were channelled in the $\langle 001 \rangle$ axis of the underlying Si(001) substrate and the scattered ions were detected in the grazing angle of 100° with respect to the direction of incidence. Figure 1(b) shows the channelled-RBS geometry and ^{16}O , ^{18}O , and Si signals in the spectra for as-deposited and annealed samples. The determined areal densities (in units of 10^{15}) for the as-deposited sample were $19.1 \text{ Zr}/\text{cm}^2$, $13.7 \text{ Si}/\text{cm}^2$, and $47.5 \text{ O}/\text{cm}^2$. After vacuum annealing, the areal densities of ^{16}O and Si remain constant within the accuracy of the measurement (5%). After $^{18}\text{O}_2$ annealing, Si areal density remains constant while ^{16}O and ^{18}O areal densities— $8.5^{16}\text{O}/\text{cm}^2$ and $37.6^{18}\text{O}/\text{cm}^2$ —reveal a very pronounced ^{16}O – ^{18}O exchange, although the total amount of O in the silicate film remained essentially constant.

O and Si were profiled with subnanometric depth resolution using narrow, isolated nuclear resonance profiling (NRP),¹¹ with the $^{18}\text{O}(p,\alpha)^{15}\text{N}$ at 151 keV ($\Gamma_R = 100 \text{ eV}$) and $^{29}\text{Si}(p,\gamma)^{30}\text{P}$ at 414 keV ($\Gamma_R \leq 100 \text{ eV}$) nuclear resonances, respectively, with 60° sample tilt.^{11,12} Normalized excitation curves for ^{18}O are shown in Fig. 2(a) and excitation curves for ^{29}Si in Fig. 2(b). These excitation curves can be converted into profiles using the program SPACES.¹³ Both vacuum- and $^{18}\text{O}_2$ -annealed samples present a concentration of Si in near-surface regions higher than the average values in the bulk of ZrSi_xO_y films. This is seen in Fig. 2(b) recalling that sensitivity to Si in NRP is almost two orders of magnitude higher than in RBS. Surface selective, far more

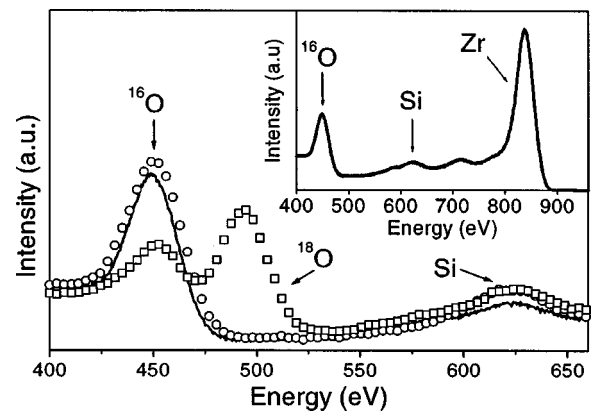


FIG. 3. Si and O signals in low energy ion scattering (ISS) spectra of 1000 eV He^+ ions. The complete spectrum for the as-deposited sample is shown in the inset. Symbols are the same as in Fig. 1.

sensitive detection of Si is accomplished with low energy ion scattering (ISS) of 1000 eV He^+ ions¹⁴ as shown in Fig. 3, confirming that the annealed samples have higher surface concentration of Si. The origin of this excess Si at the surface could be migration from the substrate across the oxide film as reported before for other high- K oxides deposited on Si.^{15–17} This transport of Si from the substrate was so far unsuspected in ZrSi_xO_y films and the present results are not sufficient to assure it. Since this may be deleterious to metal gate electrode/silicate interfaces due to silicide formation, it is imperative to understand the chemical environment of Si and of the other elements in the near-surface (and also near-interface) regions of the films, which is achieved here by angle-resolved x-ray photoelectron spectroscopy (ARXPS).

Zr $3d$, O $1s$, and Si $2p$ photoelectrons produced by Mg $K\alpha$ x rays were analyzed at different takeoff angles (Θ) between the normal to the sample surface and the axis of the energy analyzer.¹⁷ This allows a comparison of the relative intensity ratios of all species present in near-surface (surface-sensitive mode, $\Theta = 60^\circ$) and near-interface (bulk-sensitive mode, $\Theta = 25^\circ$) regions as well as at intermediate values of Θ . Zr $3d$ photoelectron spectra obtained here for the as-deposited sample were identical to those already described in the literature⁴ corresponding to the formation of Zr–O bonding in the vicinity of Si (Zr silicate) with no evidence of Zr–Si bonding. Results obtained after vacuum- and $^{18}\text{O}_2$ -annealing at different takeoff angles did not provide any evidence of modification of the Zr chemical environment.

Figure 4 shows the O $1s$ region in surface- and bulk-sensitive modes. The spectra have been fitted with two components, which are related to O–Si and O–Zr bonds, as expected for Zr silicate.⁴ The bulk-sensitive mode presents little change in relative intensities of the components for as-deposited and annealed samples, indicating chemical stability in the near-interface regions. On the other hand, the surface-sensitive mode displays an enhancement of the O–Si component in the $^{18}\text{O}_2$ -annealed sample, while in the vacuum-annealed sample there is a decrease of this component, both cases are with respect to the as-deposited sample. This implies modifications of the chemical environment of O in the near-surface region depending on the kind of thermal annealing.

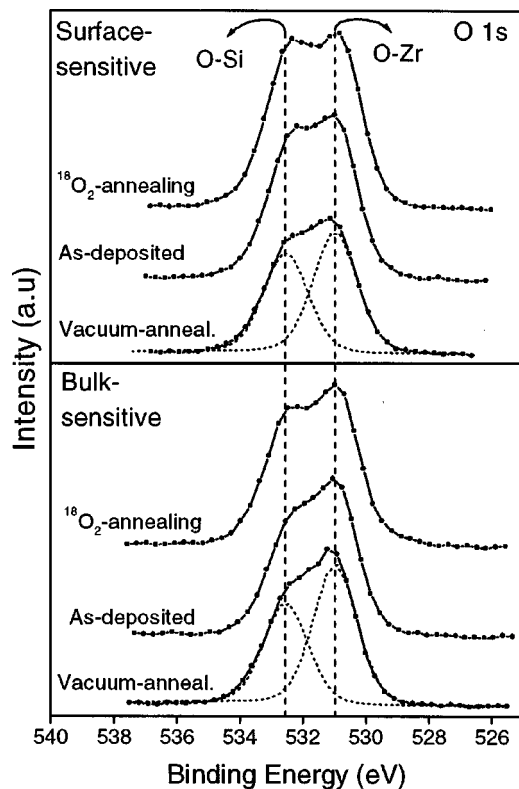


FIG. 4. O 1s region in surface sensitive ($\Theta = 60^\circ$) and bulk-sensitive ($\Theta = 25^\circ$) modes of ARXPS.

Figure 5 shows Si 2p ARXPS. The fitting procedure reveals Si–O–Zr bond⁴ (Zr silicate environment of Si) and Si–O bond (Si oxide environment in silicate network), with a marked predominance of the Si–O–Zr component. In bulk-

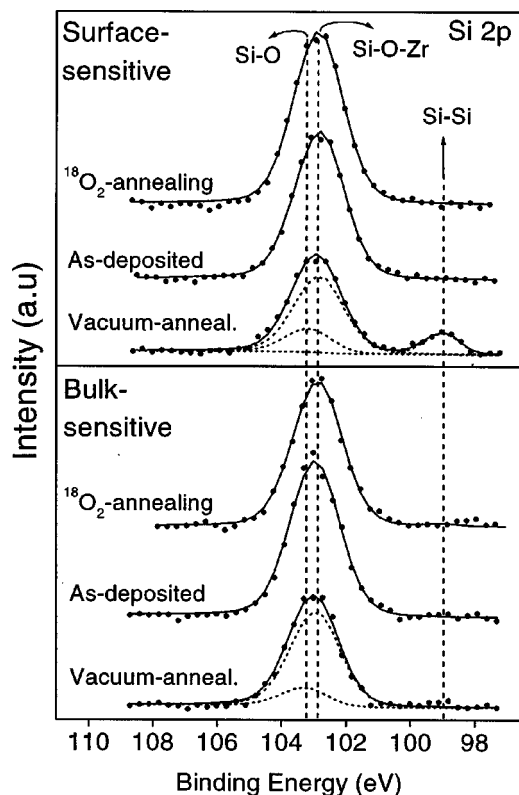


FIG. 5. Si 2p region in surface sensitive ($\Theta = 60^\circ$) and bulk-sensitive ($\Theta = 25^\circ$) modes of ARXPS.

sensitive mode, the chemical situation of Si is not significantly affected by thermal annealing. However, the surface-sensitive mode reveals a Si–Si bond (Si in a Si environment) in the vacuum annealed sample, whereas the $^{18}\text{O}_2$ -annealed sample remains essentially unchanged with respect to the as-deposited sample.

Information provided by O 1s and Si 2p XPS analysis lead to attribution of different chemical status to Si atoms that migrate and accumulate in near-surface regions after vacuum and O_2 annealing, as observed by NRP and ISS. They apparently form Si precipitates under vacuum annealing, whereas under O_2 annealing, due to the abundant offer of O, the Si precipitates are either fully or partly oxidized with the remaining been reintegrated in the Zr silicate network (with different Zr, Si, and O proportions).

In summary, this work reports experimental evidence that the interface between deposited ZrSi_xO_y films and the *c*-Si substrate remains stable, concerning atomic transport and chemical reaction, when submitted to thermal annealings at 600°C in vacuum and in $^{18}\text{O}_2$ atmosphere. A strong ^{16}O – ^{18}O exchange takes place throughout the whole silicate film during $^{18}\text{O}_2$ annealing, although without changing significantly the total amount of O in the films. On the other hand, the surface of the ZrSi_xO_y films is not stable, presenting Si migration and accumulation. In the case of vacuum annealing, the accumulated Si atoms segregate in the form of silicon precipitates. This instability may have significant deleterious consequences once a metal electrode is deposited on the Zr silicate films, either before or after vacuum annealing, since metal silicides and silicates may be formed at the electrode/dielectric interface.

¹A. I. Kingon, J.-P. Maria, and S. K. Streiffer, *Nature (London)* **406**, 1032 (2000).

²G. Timp, K. K. Bourdelle, J. E. Bower, F. H. Baumann, T. Boone, R. Cirelli, K. Evans-Lutterodt, J. Gamo, A. Ghetti, H. Gossmann, M. L. Green, D. Jacobson, S. Moccio, D. A. Muller, L. E. Ocola, M. L. O'Malley, J. Rosamilia, J. Sapjeta, P. Silverman, T. Sorsch, D. M. Tennant, W. Timp, and B. E. Weir, *Tech. Dig. Int. Electron Devices Meet.* **615** (1998).

³M. Houssa, V. V. Afanasev, A. Stesmans, and M. M. Heyns, *Appl. Phys. Lett.* **77**, 1885 (2000).

⁴G. D. Wilk, R. M. Wallace, and J. M. Anthony, *J. Appl. Phys.* **87**, 484 (2000).

⁵G. D. Wilk and R. M. Wallace, *Appl. Phys. Lett.* **76**, 112 (2000).

⁶B. H. Lee, L. Kang, R. Nieh, W.-J. Qi, and J. Lee, *Appl. Phys. Lett.* **76**, 1926 (2000).

⁷W.-J. Qi, R. Nieh, E. Dhamarajan, B. H. Lee, Y. Jeon, L. Kang, K. Onishi, and J. Lee, *Appl. Phys. Lett.* **77**, 1704 (2000).

⁸C. Chaneliere, J. L. Autran, R. A. B. Devine, and B. Balland, *Mater. Sci. Eng., R.* **22**, 269 (1998).

⁹K. J. Hubbard and D. G. Schlom, *J. Mater. Res.* **11**, 2757 (1996).

¹⁰L. C. Feldman, P. J. Silverman, J. S. Williams, T. E. Jackman, and I. Stensgaard, *Phys. Rev. Lett.* **41**, 1396 (1978).

¹¹I. J. R. Baumvol, *Surf. Sci. Rep.* **36**, 1 (1999).

¹²I. J. R. Baumvol, C. Krug, F. C. Stedile, F. Gorris, and W. H. Schulte, *Phys. Rev. B* **60**, 1492 (1999).

¹³I. Vickridge and G. Amsel, *Nucl. Instrum. Methods Phys. Res. B* **45**, 6 (1990).

¹⁴D. G. Armour, in *Methods of Surface Analysis*, edited by J. M. Walls (Cambridge University Press, Cambridge, 1989).

¹⁵J. J. Chambers and G. N. Parsons, *Appl. Phys. Lett.* **77**, 2385 (2000).

¹⁶S. Guha, E. Cartier, M. A. Gribelyuk, N. A. Bojarczuk, and M. C. Copel, *Appl. Phys. Lett.* **77**, 2710 (2000).

¹⁷C. Krug, E. B. O. da Rosa, R. M. C. de Almeida, J. Morais, I. J. R. Baumvol, T. D. M. Salgado, and F. C. Stedile, *Phys. Rev. Lett.* **85**, 4120 (2000).